

IRON K α EMISSION FROM THE LOW-LUMINOSITY ACTIVE GALAXIES M81 AND NGC 4579G. C. DEWANGAN^{1,2}, R. E. GRIFFITHS¹, T. DI MATTEO³, & N. J. SCHURCH¹*To appear in ApJ*

ABSTRACT

We report on *XMM-Newton* spectroscopy of the low-luminosity active galaxies (LLAGN) M81 and NGC 4579 both of which have known black hole masses and well-sampled spectral energy distributions (SED). The iron K α line profiles from both the LLAGN can be described in terms of two components – a narrow line at 6.4 keV and a moderately broad line (FWHM $\sim 2 \times 10^4$ km s⁻¹) arising from highly ionized, He-like or H-like species ($E \sim 6.8$ keV). We interpret the broad lines arising from an accretion disk the inner edge of which is restricted to large radii ($r_{in} \sim 100r_g$). However, the Eddington ratio, L/L_{Edd} , of these sources, is 3–4 orders of magnitude lower than that required to photo-ionize a cold disk to He-like iron. We suggest that the lines can be explained as collisionally ionized X-ray lines arising from the transition region between a hot (radiatively inefficient) flow in the inner regions and a cold disk outside $r \sim 100r_g$. The accretion flow geometry probed by our *XMM-Newton* observations is consistent with the truncated disk models proposed to explain the SED of LLAGNs.

Subject headings: accretion, accretion disks – galaxies: active – X-rays: galaxies

1. INTRODUCTION

Active galactic nuclei (AGN) typically display a ‘big blue bump’ in their optical/UV spectra interpreted as blackbody emission arising from optically thick, geometrically thin accretion disks. Their hard X-ray power-law spectrum is thought to be produced by Comptonization of the soft disk photons in a hot corona above the accretion disk (e.g.; Haardt & Maraschi 1991). Low luminosity AGN (LLAGN), emitting well below their Eddington limit ($L/L_{Edd} \leq 0.01$), typically lack the ‘big blue bump’ (e.g., Ho 1999; Di Matteo et al. 2003 for the case of M87) and for this reason it has been proposed that in these objects the accretion disk consists of two zones: an outer thin disk that extends from some large radius down to a transition radius and an inner low-radiative efficiency accretion flow close to the black hole.

Fluorescence Fe K α line emission can be a very powerful probe for the accretion flow geometry around black holes. Such lines have been interpreted as being produced through X-ray irradiation of the accretion disk; therefore the physical width of the line can serve as a trace of the inner accretion disk extent. Observations of relativistically broadened iron K α lines from some Seyfert galaxies (e.g., MCG-6-30-15 – Wilms et al 2001; Fabian et al. 2002), which require that the disk must be irradiated from an X-ray source within $6r_g$, suggests that at least in this case the accretion disk extends to the last stable orbit. It is interesting to note that MCG-6-30-15 (FWHM(H α) ~ 2200 km s⁻¹; Sulentic et al. 1998) is like narrow-line Seyfert 1 galaxies (NLS1), which are thought to be accreting at relatively high accretion rates.

In contrast, Lasota et al. (1996) suggested that the accretion disk in most LLAGN must be truncated. Gammie, Narayan, and Blandford (1999) have shown the broadband spectrum of NGC 4258 can be explained by emission from a geometrically thin accretion disk + ADAF model

with a transition radius at $\sim 10 - 100$ Schwarzschild radii (r_S). On the basis of their optical/UV continuum spectra, Quataert et al. (1999), have provided further evidence for such accretion flow geometry and showed that the spectral energy distributions of M 81 and NGC 4579 can be explained by an ADAF + disk with a transition radius at $\approx 100r_S$.

One prediction from any such models, as discussed in Quataert et al (1999), is the lack of a relativistically broadened iron K α line in the X-ray spectrum of these objects. The presence, or absence, of this feature in X-ray spectra from *Chandra* and *XMM-Newton* can therefore be used to test the accretion flow geometry proposed for LLAGN. Specifically, any detection of relativistically broad iron K α line would strongly argue against truncated disk models.

In this paper, we utilize *XMM-Newton* observations of two of the best studied LLAGN, NGC 4579 and M 81, to investigate whether the observed iron K α profiles are consistent with truncated disk models. Both NGC 4579 and M 81 show broad H α line and are classified as type 1 AGN (Barth et al. 2001; Filippenko & Sargent 1985).

2. OBSERVATION AND DATA REDUCTION

XMM-Newton observed NGC 4579 and M 81 on 12 June 2003 and 22-23 April 2001 respectively, using the European Photon Imaging Camera (EPIC), the reflection grating spectrometer (RGS), and the optical monitor (OM) instruments. The EPIC PN (Strüder et al. 2001) and MOS (Turner et al. 2001) cameras were operated in full frame mode using the thin filter for the observation of NGC 4579. For the observation of M 81, the EPIC PN was operated in small window, the MOS1 camera was operated in fast uncompressed mode and the MOS2 camera was operated in full frame mode, with the medium filter in place for all three detectors. We present the spectral data obtained from the EPIC cameras for NGC 4579 and the spectral data from the EPIC PN and MOS2 camera for M 81. The

¹ Department of Physics, Carnegie Mellon University, 5000 Forbes Avenue, Pittsburgh, PA 15213 USA

² email: gulabd@cmu.edu

³ Max-Planck-Institut für Astrophysik, Karl-Schwarzschild-St r. 1, 85740 Garching bei München, Germany

EPIC PN exposures were 22ks and 130ks for NGC 4579 and M 81, respectively.

The raw events were processed and filtered using the most recent updated calibration database and analysis software (SAS v5.4.1) available in August 2003. Events in the bad pixels file and those adjacent pixels were discarded. Only events with pattern 0–4 (single and double) for the PN and 0–12 for the MOS were selected. Light curves extracted from source free regions were examined for flaring particle background and affected exposure intervals were excluded from the rest of the analysis. This resulted in ‘good’ exposure time of 15.2 ks and ks for NGC 4579 and 71.9 ks M 81, respectively.

Source spectra were extracted from a circular region of radius $50''$ for both NGC 4579 and M 81. Associated background spectra were extracted from source free regions. The total number of source photons, detected with the PN is 4.1×10^4 for NGC 4579 and 5.44×10^5 for M 81. The source spectra were grouped to a minimum of 20 counts per spectral channel with appropriate sampling of the data (~ 3 channels per spectral resolution elements) and were analyzed using XSPEC 11.2.0 (Arnaud 1996). All the errors quoted below were calculated at 90% confidence level for one interesting parameter.

3. DETECTION OF COMPLEX IRON LINE PROFILES

In the following analysis, only the EPIC data above 2.5 keV are examined, the results presented in this paper are not critical to the soft X-ray spectrum. The soft X-ray spectrum of M 81 obtained from the RGS observation has been studied by Page et al. (2003b). For each object, at first the MOS and PN spectra were fitted separately to check for the uncertainties due to cross-calibration problems. We found generally good agreement between MOS2 and PN cameras ($\Delta\Gamma \sim 0.03$) in the 2.5–10 keV bands. However, the MOS1 data results in a flatter ($\Delta\Gamma \sim 0.15$) spectrum. These discrepancies are consistent with that found by Molendi & Sembay (2003). Therefore we present the spectral results obtained by fitting the same model jointly to the PN and MOS2 data in the 2.5–12 keV band, and allowing the relative normalizations to vary.

3.1. NGC 4579

We fit the PN and MOS2 spectrum of NGC 4579 jointly with a power-law model modified by photoelectric absorption. This fit resulted in a χ^2 of 296.6 for 253 degrees of freedom (dof). The best-fit absorption column density is consistent with the Galactic column density ($N_H = 3.1 \times 10^{20} \text{ cm}^{-2}$ along the line of sight of NGC 4579). From this simple fit, at least two iron line components are evident in the X-ray spectrum of NGC 4579. Figure 1 shows the iron $K\alpha$ line profile of NGC 4579 as the ratio of the observed PN data to the the best-fit continuum model (see below). Addition of a narrow Gaussian line at ~ 6.4 keV improved the fit significantly ($\chi^2 = 267.1$ for 251 dof). However, excess emission is seen at ~ 6.7 keV. The addition of a broad Gaussian line (model 1: power-law + narrow Gaussian + broad Gaussian) improves the joint fit significantly ($\chi^2 = 242.5$ for 249 dof), over the best-fit single Gaussian line model and also results in a better fit than the best-fit from a model consisting of an absorbed power-law and two narrow Gaussian lines ($\chi^2 = 257.0$ for

249 dof). The best-fit parameters are $\Gamma = 1.77_{-0.07}^{+0.06}$, narrow Gaussian: $E_{K\alpha,n} = 6.40$ keV (fixed), $EW = 106$ eV, broad Gaussian: $E_{K\alpha,b} = 6.79_{-0.13}^{+0.11}$ keV, $\sigma = 231_{-97}^{+102}$ eV, $EW = 287$ eV (see model 1 in Table 1).

The observed flux of NGC 4579 in the 2.5–12 keV band is $3.9 \times 10^{-12} \text{ erg cm}^{-2} \text{ s}^{-1}$, and the corresponding luminosity is $1.2 \times 10^{40} \text{ erg s}^{-1}$ (for a distance of $d = 16.7$ Mpc as measured by Pierce & Tully, 1998). An ASCA observation of NGC 4579 in 1995 showed a strong ($EW \sim 500$ eV), marginally broad, symmetrical, iron $K\alpha$ line profile at 6.73 ± 0.13 keV, while the previous 1998 observation showed a narrow line at 6.39 ± 0.09 keV ($EW \sim 260$ eV) with no clear line at ~ 6.7 keV. It appears that both the above components observed with ASCA are clearly detected in the current XMM-Newton observation.

3.2. M 81

The PN and MOS2 spectra of M81 were also fit by a power-law modified by photoelectric absorption. The best-fit absorption column density is consistent with the Galactic value ($N_H = 4.2 \times 10^{20} \text{ cm}^{-2}$). This simple fit is statistically unacceptable (χ^2 of 397.5 for 303 dof) due to significant spectral features in the iron $K\alpha$ region (see Fig. 1). The complex line profile of M 81 is not well described by a narrow Gaussian line with the power-law plus narrow Gaussian model resulting in a poor fit ($\chi^2 = 363.0$ for 303 dof). The addition of a second narrow Gaussian line at ~ 6.7 keV improves the fit significantly ($\chi^2 = 318.3$ for 301 dof). Varying the width of this line further improves the fit ($\chi^2 = 299.3$ for 300 dof). The best-fit parameters are $\Gamma_X = 1.87 \pm 0.02$, narrow Gaussian: $E_{K\alpha,n} = 6.40$ keV (fixed), $EW = 31$ eV, broad Gaussian: $E_{K\alpha,b} = 6.79_{-0.07}^{+0.06}$ keV, $\sigma = 188_{-57}^{+76}$ eV, $EW = 101$ eV.

The observed flux of M 81 in the 2.5–12 keV band is $1.2 \times 10^{-11} \text{ erg cm}^{-2} \text{ s}^{-1}$, and the luminosity in the same band is $1.8 \times 10^{40} \text{ erg s}^{-1}$ (for a distance of $d = 3.6$ Mpc; Freedman et al. 1994).

The XMM-Newton observations of M 81 confirm the previous ASCA and BeppoSAX results that detected an intrinsically broad or complex iron line centered at ~ 6.7 keV, with an equivalent width of $\sim 170 \pm 60$ eV (Ishisaki et al.1996). Neither ASCA nor XMM-Newton observations detected an absorption edge at ~ 8.6 keV, similar to that observed previously with BeppoSAX (Pellegrini et al. 2000).

4. INFERENCES FROM THE IRON LINES

Both NGC 4579 and M 81 show iron line emission with broad ($FWHM \sim 20000 \text{ km s}^{-1}$), symmetrical line profiles, in addition to narrow iron $K\alpha$ lines at 6.4 keV.

The broad iron $K\alpha$ lines cannot be easily interpreted as thermal emission from the host galaxy because the inferred thermal broadening from such a system is too small ($FWHM \sim 350 \text{ km s}^{-1}$ for a temperature of 10^8 K) to explain the widths of the observed lines. A thermal origin for the lines is further ruled out by the variability of the lines as observed by ASCA (Terashima et al. 2000).

The observed broad line from NGC 4579 and M 81 may thus arise from the accretion disk, as generally assumed in Seyfert galaxies. The broad Gaussian lines in the current models were replaced with the disk-line model of Fabian et

al. (1989) in order to test this hypothesis. This model assumes a Schwarzschild geometry and a disk emissivity that is a power-law as a function of disk radius ($\epsilon \propto r^{-q}$). The emissivity index was fixed at $q = 2.5$, the average value for Seyfert 1 galaxies derived by Nandra et al. (1997). The outer disk radius was also fixed at $1000r_g$ and the disk inclination angle i was fixed at 30 deg. The free parameters of the disk-line model were the line energy, the inner radius of the accretion disk, and the line flux. This model (model 2: power-law + narrow Gaussian + diskline) results in an acceptable fit for both AGN; $\chi^2/dof = 240.6/249$ for NGC 4579 and $\chi^2/dof = 296.3/300$ for M 81. The continuum and narrow Gaussian line parameters did not change significantly (see Table 1).

Figure 2 shows the observed PN data, the best-fit model (which includes an absorbed power law a narrow Gaussian and a diskline) and the deviations (in units of σ) for NGC 4579 and M 81. The iron $K\alpha$ profiles, shown in Fig. 1 as the ratio of observed data and the best-fit continuum model, were obtained by setting the normalizations of the narrow and broad $K\alpha$ lines to be zero. Only the ratios to the PN data are plotted in Fig. 1 for clarity. In order to evaluate the dependence of the line properties on disk inclination, we also fit the data for $i = 60$ deg. This results in $E_{diskline} = 6.70_{-0.09}^{+0.09}$ keV; $r_{in} = 232_{-117}^{+490}r_g$ for NGC 4579 and $E_{diskline} = 6.82_{-0.10}^{+0.05}$ keV; $r_{in} > 160r_g$ for M 81. Fitting accretion disk models to the data suggest that the line emitting region of the disk is truncated at an inner radius of about or greater than $100r_g$ (the narrow core to the 6.4 keV line suggests that this component must also originate at a substantial distance from the black hole).

Our best-fit model does not show any residuals indicating the presence of a substantial reflection continuum (from either neutral or partially ionized matter from a disk close to the black hole) in the spectral data of either M81 or NGC 4579 (see Fig. 2). The apparently lack of reflection continuum was also confirmed by the detailed spectral analysis of the *BeppoSAX* observation of M81 (Pellegrini 2000). It is therefore unlikely the the 6.7 keV emission is produced by reflection from an ionized disk (see also §5.2). To assess the possible origin of the ~ 6.7 keV broad feature in the spectrum of NGC 4579 as the Compton reflection emission, we fitted a Compton reflection model (*pexrav*; Magdziarz & Zdziarski 1995) along with the absorbed power-law and narrow Gaussian line model to the PN spectrum of NGC 4579. The best-fit of this reflection model results in an unrealistically large relative reflection parameter, $R = 8.2_{-1.5}^{+8.9}$ (where $R = 1$ corresponds to a solid angle of 2π subtended by the reflector) and the fit worsens ($\Delta\chi^2 = +20.7$ for an additional dof) in comparison to the best-fit obtained with the absorbed power law and double Gaussian line model (see Table 1). Thus the unphysical value of the reflection parameter and the poor quality of the fit rule out Compton reflection emission in place of the fluorescence iron $K\alpha$ emission.

Finally, a combination of multiple narrow Gaussian lines was also tested as a model to fit the complex iron line profiles observed in these sources. Three narrow Gaussian emission lines were added to the absorbed power-law model with fixed line energies of 6.4, 6.7 and 7.0 keV, corresponding to cold, He-line, and H-like iron. The fits based on this model are statistically acceptable fits (NGC 4579,

$\chi^2 = 248.5$ for 250 dof; M 81, $\chi^2 = 304.1$ for 301 dof). These are worse fits compared to the diskline models ($\Delta\chi^2 = +7.9$ and $+7.8$ for NGC 4579 and M 81, respectively) at a confidence level of 99.5% based on an F-test. With the current generation of X-ray spectroscopy satellites it is not possible to clearly distinguish between the multiple (≥ 3) narrow line and the disk-line models however, observations with, *Astro E2*, and *Constellation-X*, with their correspondingly higher spectral resolution and sensitivity will be particularly important to further investigate the complexity of these iron line profiles.

5. ORIGIN OF IRON LINE COMPLEX

Both NGC 4579 and M 81 show complex Iron $K\alpha$ features which are well described by a combination of a narrow Gaussian and either a broad Gaussian emission line, a disk-line, or a combination of narrow emission lines from multiple ionization states of iron.

5.1. The neutral, narrow iron $K\alpha$ line

Despite the good spectral resolution of the EPIC cameras, the line energies and the widths of the observed narrow $K\alpha$ lines are not well constrained. The line parameters for NGC 4579 are similar to the narrow lines commonly observed from Seyfert galaxies with *Chandra* and *XMM-Newton* (e.g., Yaqoob et al. 2001; Pounds et al. 2001), however, the strength of the narrow $K\alpha$ line is weaker in M 81, in comparison to that of 'typical' Seyfert 1 galaxies (see e.g. Page et al. 2003a). The observed narrow-lines from NGC 4579 and M 81 can be produced anywhere in the broad-line region, dusty torus, outer regions of an standard accretion disk or a disk with a flat emissivity law (Yaqoob et al. 2001,2003). The weaker narrow line of M 81 may suggest a smaller covering fraction of the material responsible for the narrow line emission in NGC 4579 than that in M 81.

5.2. The ionized, broad iron $K\alpha$ line

The widths and line center energies of the broad $K\alpha$ lines from NGC 4579 and M 81 are remarkably similar ($E \sim 6.7 - 6.8$ keV; FWHM ~ 20000 km s $^{-1}$) suggestive of both an origin in similar regions the AGN and a similarity in the ionization stages (He- or H-like iron) of the emitting material. The observed line energies are higher than those generally observed from Seyfert 1. In general, only narrow-line Seyfert 1 galaxies (NLS1s), with steep X-ray spectra, regularly show strong, highly ionized iron $K\alpha$ lines (Dewangan 2002). In such cases the lines are interpreted as being produced by reflection from material in the disk photo-ionized by the strong X-ray continuum. The physical problem with explaining the lines in M81 and NGC 4579 in a similar way is that we do not expect photoionization to be important in these low luminosity sources. For photo-ionized material, the ionization parameter can be written as $\xi = \frac{L}{nR^2}$, where L is the luminosity of ionizing photons, n is the density of the material, and R is the distance of the material from the ionizing source (Kallman & McCray 1982). For standard thin disks, Matt et al. (1993) have shown that the ionization parameter is strongly dependent on the accretion rate relative to the Eddington rate and hence can be rewritten as, $\xi \propto (L/L_{Edd})^3$. In order to ionize He-like iron, ξ should

be at least ~ 500 or $L/L_{Edd} \gtrsim 0.2$ (Matt et al. 1993). This result is consistent with the observation of highly ionized iron $K\alpha$ lines from some NLS1s as they are thought to emit a higher fraction of their Eddington luminosity (Pounds, Done, & Osborne 1995). For NGC 4579, the total nuclear luminosity of $\sim 5 \times 10^{41}$ erg s $^{-1}$ (Barth et al. 1996) and black hole mass in the range of $1.8 - 9.3 \times 10^7 M_{\odot}$ (Barth et al. 2001) correspond to $L/L_{Edd} \sim (0.5 - 2.2) \times 10^{-4}$ while Laor (2003) reported $L/L_{Edd} \sim 1.35 \times 10^{-4}$. Ho et al. (1996) found $L/L_{Edd} \sim (2 - 10) \times 10^{-4}$ for M 81 which has a black hole mass of $4 \times 10^6 M_{\odot}$. Thus the ionizing luminosity of both the LLAGNs NGC 4579 and M 81 are 3-4 orders of magnitude smaller than that required for a photo-ionized accretion disk with He-like iron. Clearly, the dominant ionization process in the disk of NGC 4579 and M 81 cannot be photo-ionization.

The widths of the ionized iron $K\alpha$ lines from NGC 4579 and M 81 (FWHM ~ 20000 km s $^{-1}$) are not as broad as the line widths predicted by models of an accretion disk extending down to the last stable orbit. Assuming Keplerian motion of the emitting material (i.e., $r \sim (c^2/v_{FWHM}^2)r_g$) the size of the broad iron $K\alpha$ line emitting material is estimated to be $\sim 150r_g$ for NGC 4579 and $\sim 230r_g$ for M 81, independent of black hole mass. Thus the majority of iron $K\alpha$ photons are not produced near the last stable orbit for a Schwarzschild ($r_{in} = 6r_g$) or a Kerr black hole ($1.235r_g \leq r_{in} < 6r_g$). The same conclusion can be drawn from the disk-line fits which resulted in $r_{in} = 50_{-21}^{+111}r_g$ for NGC 4579 and $65_{-27}^{+105}r_g$ for M 81.

Two possible scenarios that can explain the observed moderate line widths and their $\sim 6.7 - 6.8$ keV centroid energy are: (i) the accretion disk is fully ionized for $r < r_{in}$ so there are no lines arising from within this region, or (ii) the accretion disk is truncated at $r \sim r_{in}$. As discussed above, however, the accretion disk cannot be photo-ionized by irradiation, and thus must be intrinsically hot. Both (i) and (ii) then imply that the inner regions of the accretion flows in M 81 and NGC 4579 LLAGNs are likely to be different from those of typical Seyfert galaxies.

5.3. The truncated disk model

Our results are consistent with the suggestion that LLAGN have accretion disks that are truncated at some large radii and have a hot flow in the inner regions (Lasota et al. 1996; Narayan 1996; Gammie et al.; Li & Wang 2000). In particular, the inner radius $r_{in} \sim 100r_s$ of the accretion disk implied by the observed iron line width is fully consistent with the position of the truncation radius deduced from the modeling of the optical/UV spectra of M 81 and NGC 4579 by Quataert et al. (1999; assuming a geometrically-thin accretion disk and an optically thin, two-temperature ADAF in the inner regions). Note also that in this model, the continuum X-ray emission is produced in the inner region of the hot flow (from $r = 1 - 100r_s$) and is due to Comptonization of synchrotron emission from the flow.

We suggest that the relatively broad 6.7 keV lines may arise from regions of the flow close to or at the transition radius, where the hot, fully ionized flow starts cooling to connect to the outer optically thick, geometrically thin region. Using the dynamical solutions of the transition regions from a thin disk to an ADAF recently de-

rived by Manmoto et al. (2001) we can try to estimate the densities and temperatures typical for this transition region. In order for the hot flow to connect to a standard thin disk the temperature and velocity of the gas must change by orders of magnitude over a small transition region between the ADAF and the thin disk. For a transition radius of $r_{tr} \sim 100r_s$, the temperature ($T \propto c_s^2$) scales as $\sim r^{-1}$ in the inner regions, and as it approaches the transition radius, it then drops sharply from values of $T \sim 10^9$ K at $r \sim 50r_s$ to $\sim 10^8$ K at $r \sim 100r_s$ and cooler beyond. As pressure balance has to be maintained, the density of the flow increases sharply (by ~ 2 orders of magnitude) in the same range of radii, reaching values of $n_e \sim 2 \times 10^{12}$ cm $^{-3}$ at $r \sim 100r_s$. Even using the values of the flow density derived above, photo-ionization in the transition region is not likely to be important because of the low level of the ionizing hard X-ray flux, in fact, at the transition region we find that the ionization parameter $\xi \sim 1$. Instead, the observed He-like and H-like iron lines are likely to represent collisionally ionized X-ray lines produced in a hot, $T \sim 10^8$ K, transition region. Specific calculations of the emission line profiles from this region are not available at the moment and would be necessary to fully explore this hypothesis. To test this inference, therefore, we consider a simple thermal plasma model (`mekal`; Liedahl, Osterheld, & Goldstein (1995) and references therein) and fit it in combination with a power-law continuum and a narrow Gaussian emission line at 6.4 keV (fixed) to the PN and MOD spectra jointly. The density of the plasma was fixed to $n = 2 \times 10^{12}$ cm $^{-3}$ (as derived above) and no intrinsic absorption is required. The `mekal` model was convolved with a Gaussian in order to mimic the line broadening due to Keplerian motion of the plasma at the transition region. The Gaussian σ was fixed at 0.2 keV, similar to that derived for the broad Gaussian component in the double Gaussian model for the iron line (see Table 1). The model provided a good fit to the data ($\chi^2/dof = 246.4/249$ for NGC 4579 and $298.0/296$ for M 81), albeit somewhat worse than the models incorporating either a broad Gaussian or diskline. As an example, this model is shown in Figure 3 for the PN data of M 81. The best-fit parameters are $\Gamma = 1.73_{-0.11}^{+0.06}$, $kT = 8.3_{-5.6}^{+7.1}$ keV for NGC 4579 and $\Gamma = 1.87 \pm 0.04$, $kT = 8.5_{-3.0}^{+3.2}$ keV for M 81. The best-fit plasma temperatures for both the AGN are similar to that deduced above for the transition region. The power-law and the `mekal` fluxes are 2.6×10^{-12} and 1.3×10^{-12} erg cm $^{-2}$ s $^{-1}$ for NGC 4579 and 1.0×10^{-11} erg cm $^{-2}$ s $^{-1}$ and 1.3×10^{-12} erg cm $^{-2}$ s $^{-1}$, respectively.

The success of this model in reproducing the observed iron $K\alpha$ profiles suggests that the observed lines could be produced by collisional excitation in a relatively hot transition region between a hot flow and a thin disk. The truncation radii of $\sim 100r_s$ radii inferred by Quataert et al. (1999) to fit the optical/UV to X-ray SED is somewhat larger than the best-fit inner radii inferred from the diskline model fits to the iron $K\alpha$ line profile. However, it has been noted that if a standard disk is connected to an ADAF across a narrow transition layer, the gas near the transition radius must rotate with a super-Keplerian angular velocity (Abramowicz, Igumenshchev, & Lasota 1998) This means $v_{FWHM}(\text{Fe } K\alpha) > c(r_g/r_{tr})$

or $r_{tr} > r_{in} \sim (c^2/v_{FWHM}^2)r_g$. Additionally, the transition region, being hot ($\sim 10^8$ K), may not contribute the optical/UV emission which determined the truncation radius quoted by Quataert et al. (1999). Note also that ADAFs are likely to develop strong outflows (Blandford & Begelman 1999) or convection (Quataert & Gruzinov 1999; Narayan et al. 2000) which are likely to change the dynamics of the transition region.

5.4. *Alternative scenario – multiple narrow lines?*

The broad iron line components of NGC 4579 and M 81 can also be described in terms of multiple narrow emission lines from ionized iron, although with a lesser statistical significance. Such lines can arise from (i) hot thermal plasma, if present, outside the accretion disk e.g. host galaxy, or (ii) a photo-ionized accretion disk with flat emissivity law extending down to the last stable orbit (Yaqoob et al. 2003). The former process has already been ruled out due to the variability of the iron line from NGC 4579 (Terashima et al. 2000). The later possibility is unlikely due to a low ionization parameter (see §5.3). Thus the case for multiple narrow lines for the iron $K\alpha$ complexes of NGC 4579 and M 81 is poor at present.

6. CONCLUSIONS

Using the *XMM-Newton* EPIC observations, we detected complex iron line profiles from two LLAGN NGC 4579 and M 81. The line profiles are well described by a combination of a narrow neutral line and a broad Gaussian ($FWHM \sim 20000 \text{ km s}^{-1}$) or an accretion-disk line arising from highly ionized (He- or H-like) iron. The line profiles from both the AGN are remarkably similar except that the neutral iron $K\alpha$ line from M 81 is much weaker than that from NGC 4579. The main result of this work is that the broad and highly ionized iron $K\alpha$ lines from two LLAGNs NGC 4579 and M 81 are consistent with accretion disks whose inner edges are restricted to large radii $r_{in} \sim 100r_g$.

We thank an anonymous referee for the comments and suggestions on this paper. This work is based on observations obtained with *XMM-Newton*, an ESA science mission with instruments and contributions directly funded by ESA Member States and the USA (NASA). REG acknowledges NASA award NAG5-9902 in support of his Mission Scientist position on *XMM-Newton*.

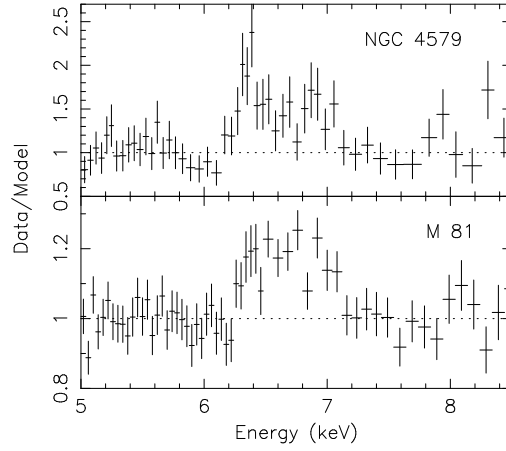


FIG. 1.— Iron $K\alpha$ line profiles of NGC 4579 and M 81 shown as the ratio of the observed PN data and the best-fit continuum model (see text).

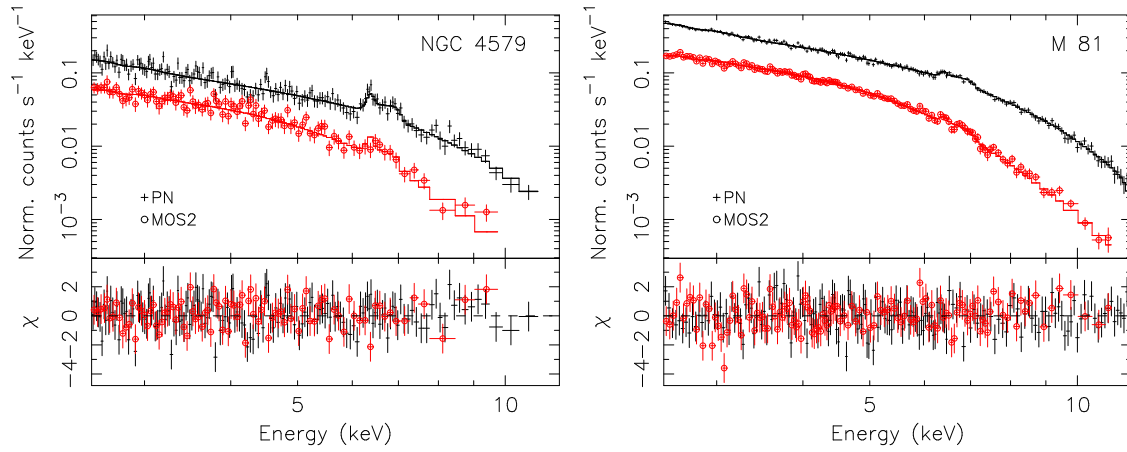


FIG. 2.— The observed EPIC PN and MOS2 spectra of NGC 4579 and M 81, the best-fit models consisting of an absorbed power-law, a narrow Gaussian, and a diskline (see text). Lower panels show the deviations of the observed data from the best-fit models.

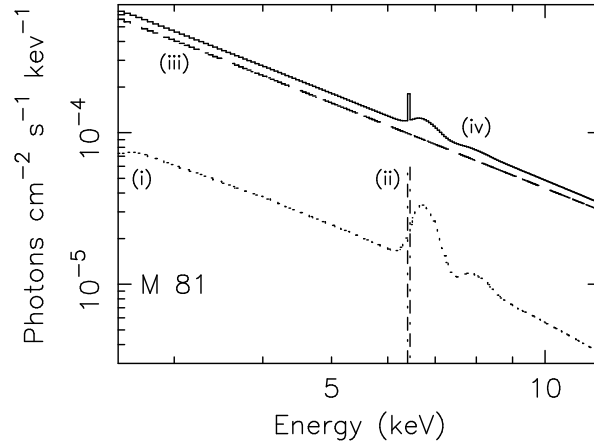


FIG. 3.— The best-fit model consisting of (i) mekal plasma model, (ii) a narrow Gaussian, and (iii) a power-law derived from the joint fit to the PN and MOS2 spectra of M 81. The model is shown for the PN data only for clarity, the model for the MOS2 data differs in relative normalization by a small fraction ($\sim 0.02\%$). The mekal model was convolved with a Gaussian of $\sigma \sim 0.2$ keV (see text)

REFERENCES

- Abramowicz, M. A., Iğumenshchev, I. V., & Lasota, J. 1998, *MNRAS*, 293, 443
- Arnaud, K. A. et al. 1985, *MNRAS*, 217, 105
- Barth, A. J., Ho, L. C., Filippenko, A. V., Rix, H., & Sargent, W. L. W. 2001, *ApJ*, 546, 205
- Barth, A. J., Reichert, G. A., Filippenko, A. V., Ho, L. C., Shields, J. C., Mushotzky, R. F., & Puchnarewicz, E. M. 1996, *AJ*, 112, 1829
- Dewangan, G. C. 2002, *ApJ*, 581, L71
- Di Matteo, T., Allen, S. W., Fabian, A. C., Wilson, A. S., & Young, A. J. 2003, *ApJ*, 582, 133
- Freedman, W. L. et al. 1994, *ApJ*, 427, 628
- Gammie, C. F., Narayan, R., & Blandford, R. 1999, *ApJ*, 516, 177
- Fabian, A. C., Rees, M. J., Stella, L., & White, N. E. 1989, *MNRAS*, 238, 729
- Ishisaki, Y. et al. 1996, *PASJ*, 48, 237
- Kaspi, S. et al. 2001, *ApJ*, 554, 216
- Liu, B. F. & Meyer-Hofmeister, E. 2001, *A&A*, 372, 386
- Lasota, J.-P., Abramowicz, M. A., Chen, X., Krolik, J., Narayan, R., & Yi, I. 1996, *ApJ*, 462, 142
- Liu, B. F., Yuan, W., Meyer, F., Meyer-Hofmeister, E., & Xie, G. Z. 1999, *ApJ*, 527, L17
- Lu, Y. & Wang, T. 2000, *ApJ*, 537, L103
- Matt, G., Fabian, A. C., & Ross, R. R. 1993, *MNRAS*, 262, 179
- Manmoto, T., Kato, S., Nakamura, K. E., & Narayan, R. 2000, *ApJ*, 529, 127
- Molendi, S., & Sembay, S. 2003, XMM-SOC-CAL-TN-0036.
- Nandra, K., George, I. M., Mushotzky, R. F., Turner, T. J., & Yaqoob, T. 1997, *ApJ*, 477, 602
- Page, K. L., O'Brien, P. T., Reeves, J. N., & Turner, M. J. L. 2003a, *ArXiv Astrophysics e-prints*, 9394
- Page, M. J., Breeveld, A. A., Soria, R., Wu, K., Branduardi-Raymont, G., Mason, K. O., Starling, R. L. C., & Zane, S. 2003b, *A&A*, 400, 145
- Pellegrini, S., Cappi, M., Bassani, L., Malaguti, G., Palumbo, G. G. C., & Persic, M. 2000, *A&A*, 353, 447
- Pounds, K. A., Done, C., & Osborne, J. P. 1995, *MNRAS*, 277, L5
- Pounds, K., Reeves, J., O'Brien, P., Page, K., Turner, M., & Nayakshin, S. 2001, *ApJ*, 559, 181
- Quataert, E., Di Matteo, T., Narayan, R., & Ho, L. C. 1999, *ApJ*, 525, L89
- Strüder, L. et al. 2001, *A&A*, 365, L18
- Terashima, Y., Kunieda, H., Misaki, K., Mushotzky, R. F., Ptak, A. F., & Reichert, G. A. 1998, *ApJ*, 503, 212
- Terashima, Y., Ho, L. C., Ptak, A. F., Yaqoob, T., Kunieda, H., Misaki, K., & Serlemitsos, P. J. 2000, *ApJ*, 535, L79
- Turner, M. J. L. et al. 2001, *A&A*, 365, L27
- Yaqoob, T., George, I. M., Nandra, K., Turner, T. J., Serlemitsos, P. J., & Mushotzky, R. F. 2001, *ApJ*, 546, 759
- Yaqoob, T., George, I. M., Kallman, T. R., Padmanabhan, U., Weaver, K. A., & Turner, T. J. 2003, *ApJ*, 596, 85

TABLE 1
BEST-FIT SPECTRAL MODEL PARAMETERS FOR NGC 4579 AND M 81.

Comp.	Parameter ^a	NGC 4579		M 81	
		model 1 ^b	model 2 ^b	model 1 ^b	model 2 ^b
PL	Γ_X	$1.77^{+0.06}_{-0.07}$	$1.77^{+0.06}_{-0.07}$	$1.86^{+0.02}_{-0.02}$	$1.86^{+0.02}_{-0.02}$
	n_{PL} ^c	$1.02^{+0.10}_{-0.09}$	$1.02^{+0.11}_{-0.09}$	$3.6^{+0.1}_{-0.1}$	$3.6^{+0.1}_{-0.1}$
Gaussian	$E_{K\alpha,n}$ (keV)	6.40(f)	6.40(f)	6.40(f)	6.40(f)
	σ (keV)	0.00(f)	0.00(f)	0.00(f)	0.00(f)
	f ^d	$4.7^{+2.3}_{-2.5}$	$4.3^{+2.5}_{-1.9}$	$3.7^{+1.6}_{-1.9}$	$4.2^{+1.6}_{-2.3}$
	EW (eV)	106	96	31	35
Gaussian	$E_{K\alpha,b}$ (keV)	$6.79^{+0.11}_{-0.13}$	–	$6.79^{+0.06}_{-0.07}$	–
	σ (eV)	231^{+102}_{-97}	–	188^{+76}_{-57}	–
	f ^d	$9.9^{+4.4}_{-3.8}$	–	$10.4^{+3.2}_{-2.6}$	–
	EW (eV)	287	–	101	–
DL	$E_{diskline}$ (keV)	–	$6.78^{+0.06}_{-0.09}$	–	$6.84^{+0.04}_{-0.07}$
	q	–	2.5	–	2.5(f)
	r_i/r_g	–	53^{+137}_{-22}	–	104^{+110}_{-61}
	r_o/r_g	–	1000(f)	–	1000(f)
	i	–	30(f)	–	30(f)
	f ^d	–	$10.0^{+3.4}_{-3.6}$	–	$10.1^{+3.0}_{-2.3}$
	EW_D (eV)	–	302	–	104
Total	χ^2_{min}/dof	242.5/249	240.6/249	299.3/300	296.3/300

^a(f) indicates a fixed parameter value.

^bmodel 1: absorbed power law + narrow Gaussian + broad Gaussian; model 2: absorbed power law + narrow Gaussian + diskline.

^c 10^{-3} photons $\text{cm}^{-2} \text{s}^{-1} \text{keV}^{-1}$ at 1 keV.

^d 10^{-6} photons $\text{cm}^{-2} \text{s}^{-1}$.